

# Osthole Suppresses Hepatocyte Growth Factor (HGF)-Induced Epithelial-Mesenchymal Transition via Repression of the c-Met/Akt/mTOR Pathway in Human Breast Cancer Cells

Chao-Ming Hung,<sup>†</sup> Daih-Huang Kuo,<sup>§</sup> Chun-Hung Chou,<sup>#</sup> Yen-Chao Su,<sup>⊥</sup> Chi-Tang Ho,<sup>⊗</sup> and Tzong-Der Way<sup>\*,#,Δ</sup>

<sup>†</sup>Department of General Surgery, E-Da Hospital, I-Shou University, Kaohsiung, Taiwan

<sup>§</sup>Graduate Institute of Pharmaceutical Technology, Tajen University, Pingtung, Taiwan

<sup>#</sup>Department of Biological Science and Technology, College of Life Sciences, China Medical University, Taichung, Taiwan

<sup>⊥</sup>Department of Food Science, Nutrition, and Nutraceutical Biotechnology, Shih Chien University, Taipei, Taiwan

<sup>⊗</sup>Department of Food Science, Rutgers University, New Brunswick, New Jersey, United States

<sup>Δ</sup>Institute of Biochemistry, College of Life Science, National Chung Hsing University, Taichung, Taiwan

**ABSTRACT:** Substantial activation of the HGF/c-Met signaling pathway is involved in the progression of several types of cancers and associated with increased tumor invasion and metastatic potential. Underlying HGF-induced tumorigenesis, epithelial to mesenchymal transition (EMT) shows a positive correlation with progression in patients. We previously determined that osthole is a potent fatty acid synthase (FASN) inhibitor. FASN is implicated in cancer progression and may regulate lipid raft function. We therefore examined whether osthole could block HGF-induced tumorigenesis by disrupting lipid rafts. Here, we found that osthole could abrogate HGF-induced cell scattering, migration, and invasion in MCF-7 breast cancer cells. Osthole also effectively inhibited the HGF-induced decrease of E-cadherin and increase of vimentin via down-regulation of phosphorylated Akt and mTOR. Interestingly, osthole blocked HGF-induced c-Met phosphorylation and repressed the expression of total c-Met protein in MCF-7 cells. In addition, C75, a pharmacological inhibitor of FASN, repressed the expression of total c-Met protein in MCF-7 cells. Consistent with a role for FASN, loss of c-Met in cells treated with osthole was prevented by the exogenous addition of palmitate. Briefly, our result suggests a connection between FASN activity and c-Met protein expression and that osthole is a potential compound for breast cancer therapy by targeting the major pathway of HGF/c-Met-induced EMT.

**KEYWORDS:** osthole, epithelial-mesenchymal transition, c-Met, Akt, mTOR

## INTRODUCTION

Tumor invasion and metastasis are the main cause of death in cancer patients. The transition of the stationary cancer cells to a motile mesenchymal-like phenotype is a milestone of carcinoma progression during the invasive and metastatic phases. Therefore, therapeutic approaches to block this process are urgently needed.<sup>1</sup> Epithelial to mesenchymal transition (EMT) is a vital process in the conversion of early-stage tumors into invasive malignancies.<sup>2</sup> EMT is thought to be important in the disassembly of cell–cell junctions and eventual invasion of the basement membrane, a prerequisite for metastasis.<sup>3</sup> In addition to cancer progression and invasive and metastatic phases, EMT also contributes to emergence of cancer stem cells.<sup>4,5</sup>

The c-Met receptor tyrosine kinase, which is the receptor for hepatocyte growth factor (HGF), is expressed at elevated levels in 15–20% of human breast cancers and is a prognostic factor for poor outcome.<sup>6,7</sup> The HGF/c-Met signaling axis is a major contributor to the promotion of EMT. Upon binding of its ligand HGF, c-Met is phosphorylated and subsequently activates different signaling pathways involved in proliferation, motility, migration, and invasion.<sup>8</sup> High levels HGF in the serum of breast cancer patients is also correlated with a shorter disease-free interval after surgery and a higher tumor/lymph node/metastasis score.<sup>9</sup> Epigallocatechin-3-gallate (EGCG) and luteolin have been

identified as inhibitors of HGF-induced activation of tumorigenesis by blocking c-Met phosphorylation and the downstream cascade, including suppressing the phosphorylation of Akt and mammalian target of rapamycin (mTOR).<sup>10,11</sup>

Plant-derived natural products have been a global trend toward the use of natural matters present in fruits, vegetables, and herbs as cancer chemopreventive agents. Recently, numerous chemopreventive constituents have been isolated and/or synthesized and evaluated for their efficacy in a variety of biological assays.<sup>12</sup> The dried fruits of *Cnidium monnieri* (L.) Cusson, a well-known traditional Chinese medicine, have a variety of pharmacological and biological uses and are considered to have therapeutic applications. Osthole, an active constituent isolated from the dried fruits of *C. monnieri* (L.) Cusson, has many biological functions, including antiosteoporotic,<sup>13</sup> antihepatic,<sup>14</sup> antiallergic,<sup>15</sup> antiseizure,<sup>16</sup> and antiproliferative functions.<sup>17</sup> Osthole has received considerable attention recently because of its significant and diverse pharmacological and biological uses, which make it a very promising natural lead

**Received:** May 30, 2011

**Revised:** August 1, 2011

**Accepted:** August 1, 2011

**Published:** August 01, 2011

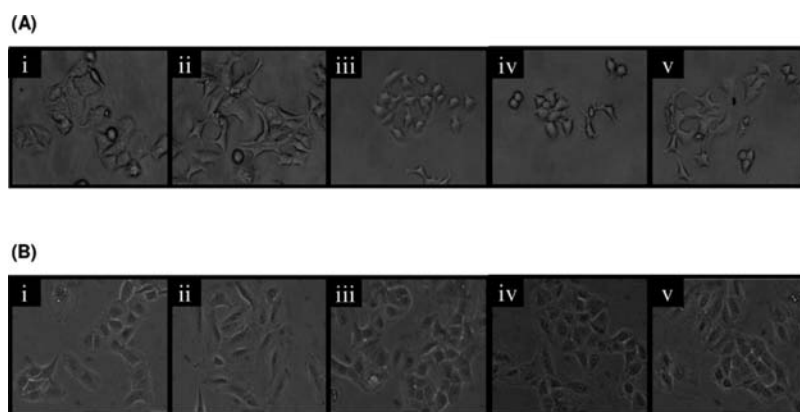


**Figure 1.** Osthole pretreatment blocks HGF-induced cell scattering. (A) MCF-7 breast cancer cells were pretreated with DMSO (i) or increasing osthole concentrations (iii, 10  $\mu$ M; iv, 20  $\mu$ M; and v, 40  $\mu$ M) for 8 h prior to HGF stimulation (ii, 33 ng/mL) for 18 h. (B) MCF-7 cells were incubated with DMSO (i) or 20  $\mu$ M osthole for 1 h (iii), 4 h (iv), or 8 h (v) prior to HGF stimulation (ii, 33 ng/mL). EMT was examined by phase contrast photomicrographs.

compound for new drug discovery. Our previous study determined that osthole was found to be effective in suppressing fatty acid synthase (FASN) expression in HER2-overexpressing breast cells.<sup>18</sup>

Lipid rafts are plasma membrane microdomains enriched in sphingolipid and cholesterol that coordinate and regulate varieties of cellular signaling in part through compartmentalization of growth factor receptors. FASN is the sole enzyme responsible for the synthesis of long-chain saturated fatty acids and may play a role in regulating the activity of lipid rafts.<sup>32</sup> Since we previously determined that osthole has a potent inhibitory effect on lipogenesis, we have further examined whether osthole could block HGF/c-Met-mediated cancer progression by disrupting lipid rafts. In this study, we provided evidence and demonstrated that osthole could inhibit HGF/c-Met signaling by blocking the downstream Akt and mTOR phosphorylation cascade and effectively abrogating HGF/c-Met-induced cell scattering and invasion in MCF-7 cells.

## MATERIALS AND METHODS

**Cell Lines and Cell Cultures.** The human breast cancer cell lines used in this study were MCF-7, MDA-MB-453, MDA-MB-231, and BT-20. All cell lines were purchased from American Type Culture Collection (Manassas, VA). All cell lines were grown in DMEM/F12 supplemented with 10% fetal bovine serum (FBS). Cells were grown in a humidified incubator at 37 °C under 5% CO<sub>2</sub> in air. Cell culture materials were obtained from Invitrogen (Burlington, ON, Canada).

**Reagents and Antibodies.** Osthole, LY294002, C75, and palmitate were purchased from Sigma Chemical Co. (St. Louis, MO). HGF was purchased from Invitrogen (Carlsbad, CA) and dissolved in PBS (137 mM NaCl, 2.7 mM KCl, 4.3 mM Na<sub>2</sub>HPO<sub>4</sub>·7H<sub>2</sub>O, and 1.4 mM KH<sub>2</sub>PO<sub>4</sub> at pH 7.4) with 0.1% BSA. Primary antibodies phospho-c-Met (Y1234/35), phospho-Erk (T202/Y204), phospho-Akt (S473), phospho-mTOR (S2448), c-Met, Erk, Akt, mTOR, E-cadherin, and  $\beta$ -actin were purchased from Cell Signaling Technology (Beverly, MA). Primary vimentin was purchased from Abcam Inc. (Cambridge, MA). Secondary antibodies, HRP-conjugated goat anti-mouse IgG and goat anti-rabbit IgG, were obtained from Millipore (Billerica, MA).

**Scattering Assay.** MCF-7 cells ( $2 \times 10^4$ ) were seeded in each well of a 24-well plate and incubated in a 37 °C incubator with 5% CO<sub>2</sub> overnight. MCF-7 cells were pretreated with the indicated concentrations of osthole for the appropriate time. HGF was added to each well

with the final concentration of 33 ng/mL.<sup>11</sup> Cells were then incubated at 37 °C for 18 h. Representative photographs were taken at 200 $\times$  magnification using a Nikon TE2000-U inverted microscope.

**Wound Healing Assay.** MCF-7 cells ( $4.5 \times 10^5$ ) were plated on a 6-well plate to form a confluent monolayer in serum-containing media. The monolayer was pretreated with 20  $\mu$ M osthole for 8 h before being scratched. The monolayers were scratched by a plastic tip and washed by PBS to remove cell debris. Half-percent serum-containing DMEM/F12, 20  $\mu$ M osthole, and 33 ng/mL HGF were then added to each well, and the scratched monolayer was incubated in a 37 °C incubator with 5% CO<sub>2</sub> for 24 h. Wound closure was measured in 10 random fields at 200 $\times$  magnification using Image-Pro Express software and a Nikon TE2000-U inverted microscope. Data of three independent experiments were analyzed by *t* test using GraphPad Prism 5 software. The distance between groups was considered to be statistically significant when *p* < 0.05.

**In Vitro Invasion Assay.** A matrigel invasion assay was performed in 24-well transwell culture plates. Briefly, 25  $\mu$ L of BD Matrigel Basement Membrane Matrix (BD Biosciences, Los Angeles, CA) was resolved at 4 °C overnight and coated on the transwell insert membrane. The inserts were then incubated at 37 °C for 30 min to gel. After matrigel coating,  $2 \times 10^4$  MCF-7 cells in 100  $\mu$ L of DMEM/F12 medium with 0.1% serum and 20  $\mu$ M osthole were added to the top chamber. Five hundred microliters of serum-containing DMEM/F12 and 33 ng/mL HGF were plated in the bottom chamber. The cells were incubated in a 37 °C incubator with 5% CO<sub>2</sub> for 24 h. After incubation, medium was aspirated, and noninvading cells were scrubbed by a wet cotton swab. The cells were washed by PBS and fixed by 4% paraformaldehyde at room temperature for 15 min. Fixed cells were washed three times by PBS and stained by 0.5% Toluidine Blue O (Sigma-Aldrich, St. Louis, MO) in 2% Na<sub>2</sub>CO<sub>3</sub> for 10 min. Excess stain was removed by three washings with distilled water. The invading cells were counted in five random fields at 400 $\times$  magnification. Three independent experiments were conducted, and data were analyzed by *t* test using GraphPad Prism 5 software. The distance between groups was considered to be statistically significant when *p* < 0.05.

**Western Blot Analysis.** Cells ( $2 \times 10^6$ ) were seeded onto a 100 mm tissue culture dish containing 10% FBS DMEM/F12 and cultured for 24 h. Then cells were incubated in 10% FBS DMEM/F12 treated with various agents as indicated in the figure captions. After treatment, cells were placed on ice, washed with cold PBS, and lysed in lysis buffer. Western blot was done as described previously.<sup>19</sup>

**Confocal Microscopy.** After treatment, cells were fixed with methanol, blocked with 3% bovine serum albumin, first stained with anti-E-cadherin or anti-vimentin monoclonal antibody and then

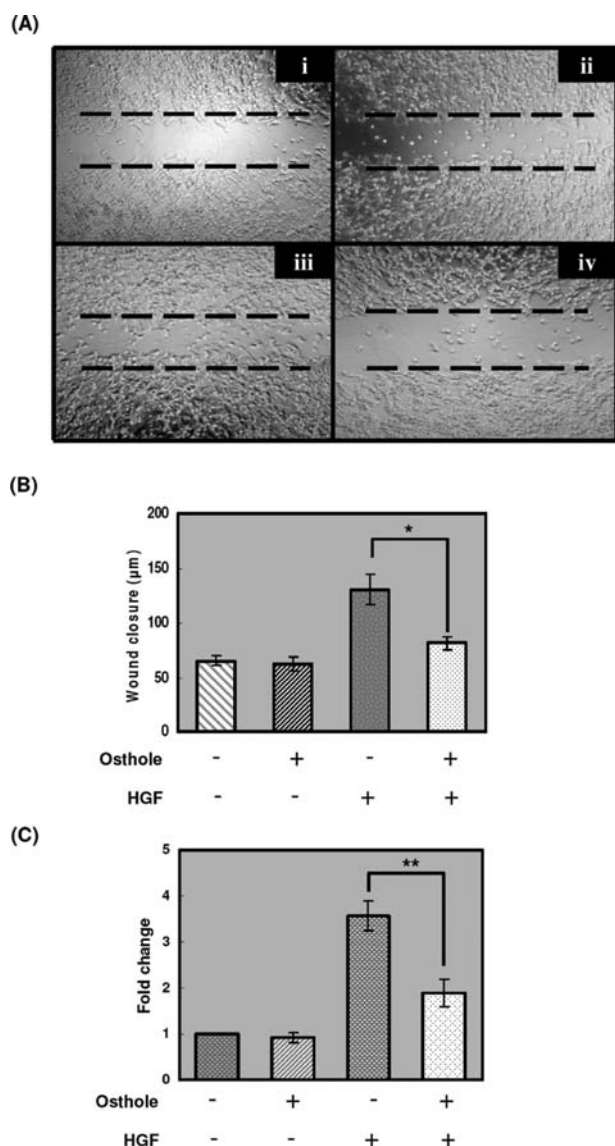


**Figure 2.** Effects of osthole on HGF-induced cell migration and invasion. (A) For wound healing assay, confluent MCF-7 monolayer was pretreated with DMSO (i) or 20  $\mu\text{M}$  osthole (ii and iv) for 8 h. Cells were then scratched by pipet tips and washed to remove the debris. Fresh medium containing 0.5% serum with DMSO (i) or with 20  $\mu\text{M}$  osthole (ii and iv) was added. Cells were then incubated alone or with HGF (iii and iv, 33 ng/mL) for 24 h. Dashed lines indicate the cell edges at  $T_0$  point. Representative pictures are shown. (B) HGF-induced cell motility was determined by measuring the closure of wounds (micrometers). Data were plotted as the mean  $\pm$  SD ( $n = 3$ ). Osthole significantly inhibited HGF-induced cell motility (\*,  $p < 0.05$ ). (C) After matrigel coating,  $2 \times 10^4$  MCF-7 cells were cultured in 0.1% serum-containing DMEM  $\pm$  20  $\mu\text{M}$  osthole in the 24-well transwell chambers. Five hundred microliters of serum-containing DMEM  $\pm$  33 ng/mL HGF was plated in the lower chamber. The cells were incubated for 24 h. Invading cells were then fixed, stained with toluidine blue, and counted in five random fields. Three independent experiments were conducted, and data were analyzed by  $t$  test using GraphPad Prism 5 software. The number of control cells was set to 1. Treatment of osthole reduced MCF-7 invasion induced by HGF (\*,  $p < 0.05$ ).

FITC-conjugated anti-mouse IgG antibody. Nuclear staining was done with DAPI. Cells were imaged with a Leica TCS SP2 spectral confocal system.

## RESULTS

**Osthole Blocked HGF-Induced Scattering of Breast Cancer Cells.** The activation of HGF/c-Met signaling significantly caused polarization of cell shape in MCF-7 cells (Figure 1Aii,1Bii). To determine if osthole, a known FASN inhibitor, also affected the HGF-induced phenotypic change, MCF-7 cells were pretreated with osthole for 8 h over a range of osthole concentrations prior to stimulation with HGF (33 ng/mL) for 18 h. Osthole blocked HGF-induced scattering in a dose-dependent fashion (Figure 1Aiii–v). To address this pretreatment time-dependent effect, we pretreated cells with 20  $\mu\text{M}$  osthole for various periods of time from 1 to 8 h prior to HGF addition. An increase in inhibition of HGF-induced scattering was observed beginning at 1 h of osthole pretreatment with a greater percentage of cells remaining adherent in colonies with 8 h of pretreatment time (Figure 1Biii–v).

**Osthole Blocked HGF-Induced Cell Migration and Invasion.** We further examined whether osthole also affected HGF-induced cell migration. We pretreated confluent MCF-7 cells with 20  $\mu\text{M}$  osthole for 8 h; cells were scratched by pipet tips and washed to remove the debris, followed by the addition of fresh medium containing 0.5% serum with 20  $\mu\text{M}$  osthole. Cells were then incubated with 33 ng/mL HGF for 24 h. HGF-induced cell migration was determined by measuring wound closure. Dot lines indicated the edges at  $T_0$  point (Figure 2A). There is no effect for cells treated with osthole alone (Figure 2Aii). Compared to cells treated with DMSO (Figure 2Ai), HGF significantly induced cell migration (Figure 2Aiii). Notably, the HGF-induced cell migration was abrogated in the presence of osthole (Figure 2Aiv). Wound closure was measured in 10 random fields at 200 $\times$  magnification using Image-Pro Express software. The data of cell motility, obtained from Figure 2A, were plotted as the mean  $\pm$  SD (Figure 2B). A modified invasion assay was performed to further determine whether osthole was capable of blocking HGF-induced invasion. MCF-7 cells ( $2 \times 10^4$ ) were plated on top of a matrigel-coated 24-well transwell chamber. Cells were cultured in 0.1% serum-containing DMEM/F12, 33 ng/mL HGF, and 20  $\mu\text{M}$  osthole for 24 h. Invading cells were then fixed, stained with toluidine blue, and counted in five random fields. The number of invasive cells induced by HGF was 3.4-fold that of DMSO control or osthole alone. Treatment of cells with 20  $\mu\text{M}$  osthole significantly decreased the number of HGF-induced invasive cells to 1.8-fold compared to control cells. Consistent with results obtained from Figure 2B, treatment of osthole reduced MCF-7 invasion induced by HGF (Figure 2C).

**Osthole Suppressed HGF-Induced EMT by Down-regulation of Vimentin and Up-regulation of E-Cadherin.** A number of molecules have served as epithelial or mesenchymal markers since the early 1980s.<sup>20</sup> Down-regulation of E-cadherin and up-regulation of vimentin are markers of EMT. To further clarify whether abolishment of HGF-induced scattering, migration, and invasion in osthole-treated MCF-7 cells resulted from altering the processes of EMT, we examined the expression of EMT marker proteins vimentin and E-cadherin. As shown in Figure 3, the expression of vimentin was increased, whereas the expression of E-cadherin was decreased when cells were activated by HGF. Pretreatment with osthole significantly suppressed the HGF-induced up-regulation of vimentin and the down-regulation of E-cadherin in a dose- and time-dependent manner (Figure 3A,B). To confirm that osthole suppressed the HGF-induced up-regulation of vimentin and down-regulation of E-cadherin, cells

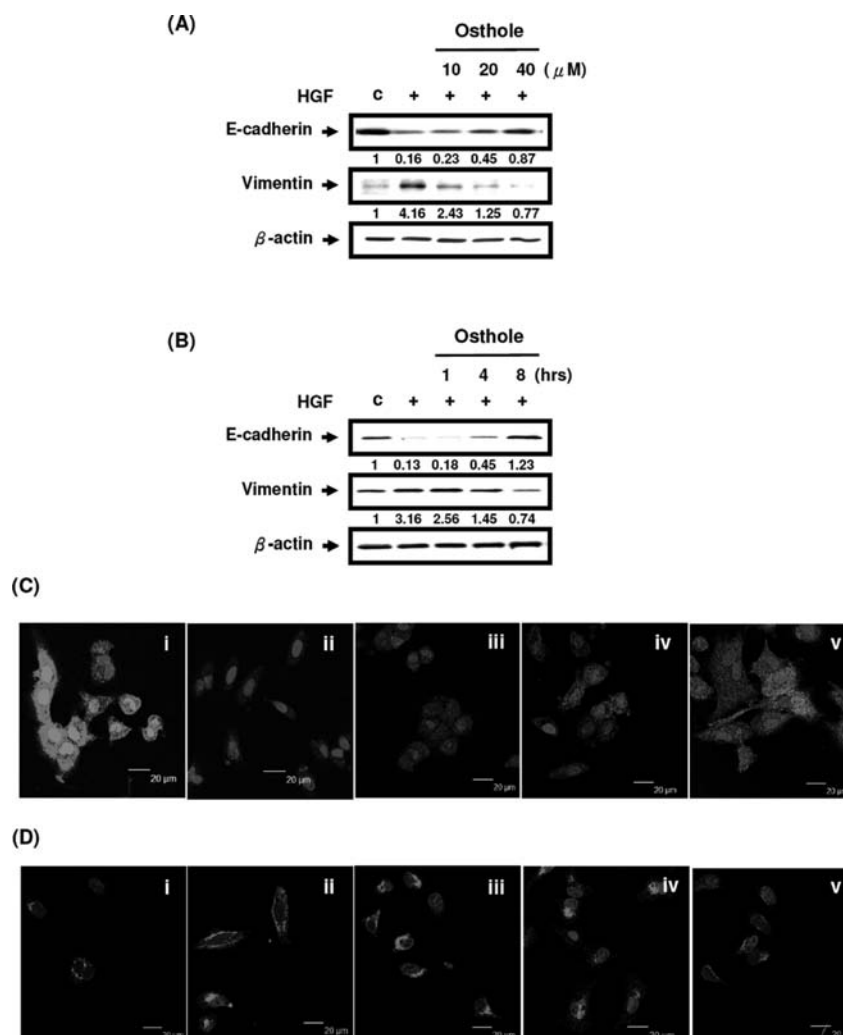


**Figure 3.** Osthole inhibits the HGF-induced EMT in MCF-7 cells. (A) MCF-7 cells were pretreated with DMSO (control) or increasing osthole concentrations for 8 h prior to HGF stimulation (33 ng/mL) for 18 h. (B) MCF-7 cells were incubated with DMSO (control) or 20  $\mu$ M osthole for 1, 4, or 8 h prior to HGF stimulation (33 ng/mL) for 18 h. The cells were then harvested and lysed for the detection of E-cadherin, vimentin, and  $\beta$ -actin. Western blot data presented are representative of those obtained in at least three separate experiments. The values below the figures represent change in protein expression normalized to  $\beta$ -actin. (C) MCF-7 cells were incubated with DMSO (i) or 20  $\mu$ M osthole for 1 h (iii), 4 h (iv), or 8 h (v) prior to HGF stimulation (ii, 33 ng/mL) for 18 h. Cells were fixed, permeabilized, and stained with anti-E-cadherin monoclonal antibody (green) and DAPI (blue). Cells were analyzed by confocal microscopy. (D) MCF-7 cells were incubated with DMSO (i) or 20  $\mu$ M osthole for 1 h (iii), 4 h (iv), or 8 h (v) prior to HGF stimulation (ii, 33 ng/mL) for 18 h. Cells were fixed, permeabilized, and stained with anti-vimentin monoclonal antibody (green) and DAPI (blue). Cells were analyzed by confocal microscopy.

were imaged using confocal microscopy. As shown in Figure 3C,D, confocal microscopy using E-cadherin and vimentin antibody indicated that HGF treatment resulted in up-regulation of vimentin (Figure 3Dii) and down-regulation of E-cadherin (Figure 3Cii). Pretreatment with osthole for various periods of time significantly suppressed the HGF-induced up-regulation of vimentin (Figure 3Diii–v) and down-regulation of E-cadherin (Figure 3Ciii–v) in a time-dependent manner.

**Osthole Pretreatment Was Required for Inhibition of c-Met/Akt/mTOR Pathway.** To determine if osthole affected HGF/c-Met signaling pathways, thus blocking cell scattering and motility, we treated MCF-7 cells with indicated concentrations of osthole for the appropriate time prior to HGF treatment for 20 min. The protein lysates from individual treatments were harvested and subjected to Western blot analysis. As shown in Figures 4A and 5A, Western blot analysis of whole cell lysates

using antibodies specific for c-Met phosphorylation showed that HGF induced c-Met phosphorylation at tyrosine residues 1234/1235 (the kinase domain). Pretreatment with osthole blocked phosphorylation of c-Met in a time- and dose-dependent manner (Figures 4A and 5A). Moreover, Western blot analysis revealed that osthole effectively blocked phosphorylation of Akt and mTOR induced by HGF in a time- and dose-dependent manner (Figures 4B and 5B). The RAF-MEK-ERK pathway has been shown to be required for HGF-induced EMT.<sup>21</sup> Conversely, HGF-mediated activation of MAP kinases, Erk, was not affected by osthole pretreatment (Figures 4C and 5C). In summary, osthole was capable of blocking HGF-induced signaling via specific repression of activation of the c-Met/Akt/mTOR pathway.

**Selective PI3K Inhibitor Inhibited HGF-Induced EMT, Cell Migration, and Invasion.** To confirm whether the AKT/mTOR is the major pathway to induce EMT while cells were activated by

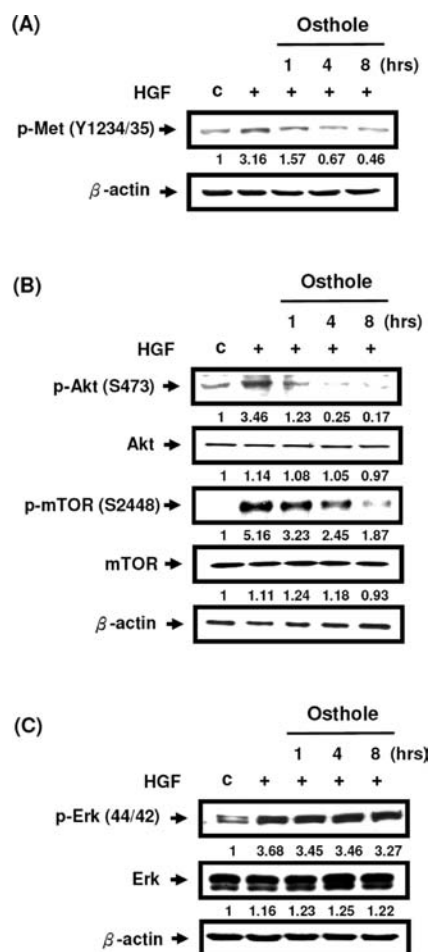


**Figure 4.** Osthole blocks HGF-induced c-Met/Akt/mTOR pathway in a time-dependent manner. MCF-7 cells were incubated with DMSO (control) or 20  $\mu$ M osthole for 1, 4, or 8 h prior to HGF stimulation (33 ng/mL) for 20 min. (A) The cells were then harvested and lysed for the detection of p-Met and  $\beta$ -actin. (B) The cells were then harvested and lysed for the detection of p-Akt, Akt, p-mTOR, mTOR, and  $\beta$ -actin. (C) The cells were then harvested and lysed for the detection of p-Erk, Erk, and  $\beta$ -actin. Western blot data presented are representative of those obtained in at least three separate experiments. The values below the figures represent change in protein expression normalized to  $\beta$ -actin.

HGF, we used the PI3K inhibitor, LY294002, to determine if inhibition of the AKT/mTOR pathway repressed the HGF-induced EMT, cell migration, and invasion. MCF-7 cells were pretreated with 10  $\mu$ M LY294002 for 1 h and then treated with HGF for 18 h. Similar to the pretreatment with osthole, cells pretreated with LY294002 significantly inhibited HGF-induced EMT (Figure 6A), cell migration (Figure 6B), and invasion (Figure 6C). Compared to the pretreatment with LY294002 or osthole alone, a pretreatment with the combination of LY294002 and osthole more significantly inhibited HGF-induced EMT (Figure 6A), cell migration (Figure 6B), and invasion (Figure 6C). Together, these data suggest that osthole suppresses HGF-induced EMT, cell migration, and invasion via repression of the c-Met/Akt/mTOR pathway in human breast cancer cells.

**Pretreatment with Osthole Induced a Loss of c-Met Most Likely through the Inhibition of FASN.** To further investigate the mechanism of osthole-mediated decrease in HGF-mediated

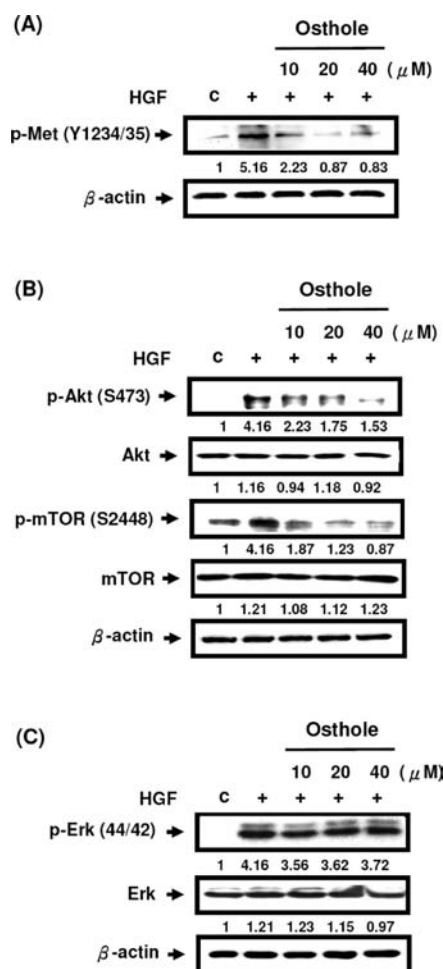


**Figure 5.** Osthole blocks HGF-induced c-Met/Akt/mTOR pathway in a dose-dependent manner. MCF-7 breast cancer cells were pretreated with DMSO (control) or increasing osthole concentrations (10, 20, and 40  $\mu$ M) for 8 h prior to HGF stimulation (33 ng/mL) for 20 min. (A) The cells were then harvested and lysed for the detection of p-Met and  $\beta$ -actin. (B) The cells were then harvested and lysed for the detection of p-Akt, Akt, p-mTOR, mTOR, and  $\beta$ -actin. (C) The cells were then harvested and lysed for the detection of p-Erk, Erk, and  $\beta$ -actin. Western blot data presented are representative of those obtained in at least three separate experiments. The values below the figures represent change in protein expression normalized to  $\beta$ -actin.

c-Met activity, we performed Western blot analysis using whole cell lysates from MCF-7 cells treated with osthole for various times. Figure 7A shows that osthole caused a reduction in the level of total c-Met protein beginning as early as 6 h. Because luteolin is a known FASN inhibitor, we predict that a specific FASN inhibitor, C75, may also induce a loss of c-Met expression. As seen in Figure 7B, the addition of C75 resulted in the loss of c-Met similar to that observed for osthole treatment. To more directly determine the role of FASN in controlling c-Met levels, the addition of palmitate, the end product of FASN catalytic activity, prevented osthole-induced c-Met loss in a dose-dependent manner (Figure 7C). These experiments suggest a potential link between FASN activity and c-Met expression levels. To confirm the generality of these findings, we examined several additional breast cancer cell lines, including MDA-MB-453, MDA-MB-231, and BT20. Osthole treatment reduced c-Met expression in all cell lines tested (Figure 7D), suggesting that the

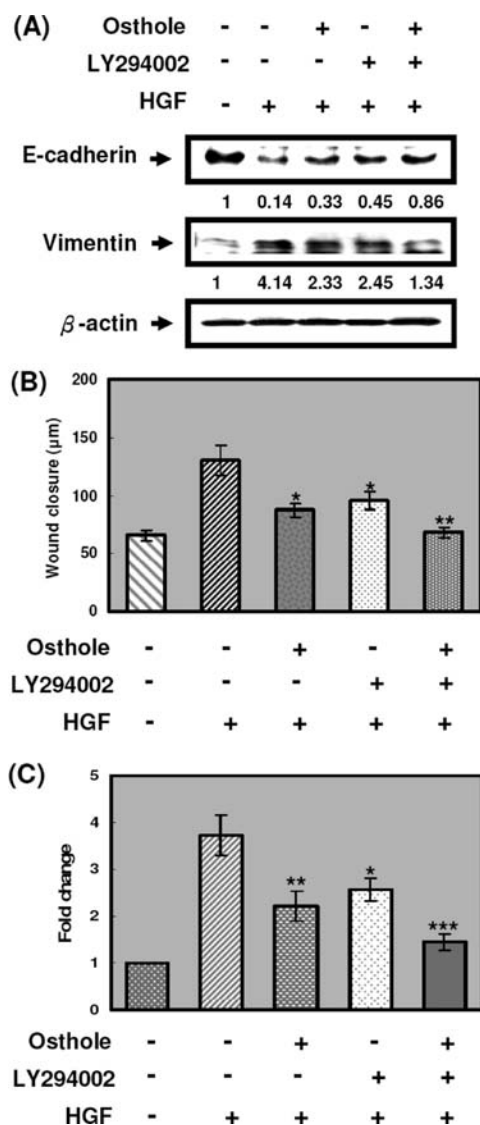


**Figure 6.** Effects of selective PI3K inhibitor inhibited HGF-induced EMT, cell migration, and invasion. MCF-7 cells were pretreated with 20  $\mu$ M osthole, 10  $\mu$ M LY294002, or a combination of 10  $\mu$ M LY294002 and 20  $\mu$ M osthole for 8 h and then treated with HGF for 18 h. (A) The cells were then harvested and lysed for the detection of E-cadherin, vimentin, and  $\beta$ -actin. Western blot data presented are representative of those obtained in at least three separate experiments. The values below the figures represent change in protein expression normalized to  $\beta$ -actin. (B) Cell motility was determined by measuring wound closure (micrometers). Data were plotted by the mean  $\pm$  SD ( $n = 3$ ). Osthole, LY294002, or a combination of LY294002 and osthole significantly inhibited HGF-induced cell motility (\*,  $p < 0.05$ ; \*\*,  $p < 0.01$ ). (C) After matrigel coating,  $2 \times 10^4$  MCF-7 cells were cultured in 0.1% serum-containing 20  $\mu$ M osthole, 10  $\mu$ M LY294002, or a combination of 10  $\mu$ M LY294002 and 20  $\mu$ M osthole in the 24-well transwell chambers. Five hundred milliliters of serum-containing 33 ng/mL HGF was plated in the lower chamber. The cells were incubated for 24 h. Invading cells were then fixed, stained with toluidine blue, and counted in five random fields. The experiment was repeated three times. The number of the control cells was set to 1. Treatment of osthole, LY294002, or a combination of LY294002 and osthole reduced MCF-7 invasion induced by HGF (\*,  $p < 0.05$ ; \*\*,  $p < 0.01$ ; \*\*\*,  $p < 0.001$ ).

observed effects of osthole on c-Met receptor levels were not cell context dependent.

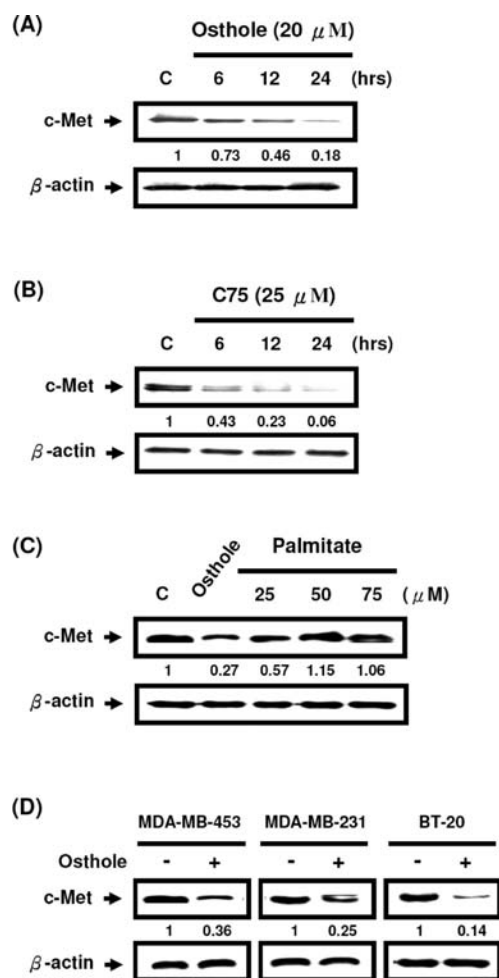


**Figure 7.** Osthole reduces c-Met levels through inhibition of FASN. (A) MCF-7 cells were treated with DMSO or 20  $\mu$ M osthole for 6, 12, or 24 h. (B) MCF-7 cells were treated with DMSO or 25  $\mu$ M C75 for 6, 12, or 24 h. (C) MCF-7 cells were pretreated with 25, 50, or 75  $\mu$ M palmitate prior to incubation with 20  $\mu$ M osthole for 12 h. (D) Human breast cancer cell lines MDA-MB-453, MDA-MB-231, and BT-20 were treated for 12 h with DMSO (-) or 20  $\mu$ M osthole (+). For each experiment, whole cell lysates were collected and probed by Western blot analysis using c-Met and  $\beta$ -actin antibodies. Western blot data presented are representative of those obtained in at least three separate experiments. The values below the figures represent change in protein expression normalized to  $\beta$ -actin.

## DISCUSSION

The well-characterized activities of HGF/c-Met pathway — proliferation, invasion, angiogenesis, and antiapoptosis — delineate the stages at which a molecule may participate in tumor progression.<sup>22–24</sup> Recently, some phytochemicals have been discovered to have potent inhibitory activity against growth factor signaling pathways, including HGF/c-Met.<sup>10,11,25</sup> In this study, we investigated the effects of osthole on the HGF/c-Met signaling axis and found that it blocked c-Met signaling through inhibition of FASN, leading to a reduction in c-Met protein levels.

Previous studies demonstrated that treatment with transforming growth factor- $\beta$  (TGF- $\beta$ ) or ectopic expression of E-cadherin repressors such as Twist or Snail can induce EMT and also confer stem cell-like properties in immortalized human

mammary epithelial cells, providing the first link of EMT and “stemness”.<sup>5</sup> Accordingly, inhibition of EMT could be a strategy not only to combat cancer metastasis but also to conquer the drug resistance caused by cancer stem cells. A selective inhibitor of cancer stem cells, salinomycin, could significantly reduce the proportion of epithelial cancer stem cells and enhance epithelial gene expression, although the detailed mechanism remains elusive.<sup>26</sup> Moreover, HGF could costimulate Wnt and Akt activities and modulate the features of colon cancer stem cells, suggesting the HGF/c-Met signaling pathway could be a therapeutic target.<sup>27</sup> The potential application of osthole to cancer stem cells, particularly to breast cancer, can be suggested.

Herein, in the presence of HGF, MCF-7 breast cancer cells lose cell–cell adhesions and acquire a motile phenotype. Pre-treatment with osthole blocks HGF-induced scattering and causes changes in cell morphology (reduction in stress fibers and cell flattening). Similar to other known compounds, such as EGCG or luteolin, which can inhibit HGF-induced migration and invasion in DU145 cells, osthole has the same effects in MCF-7 breast cancer cells.<sup>10,11</sup> Actin stress fibers are important for cell motility, and it is possible that the disruption of actin stress fibers caused by osthole treatment may account for this compound's ability to block HGF-induced scattering and motility. However, the exact mechanism will remain to be determined. HGF stimulated phosphorylation of c-Met, Akt, Erk, and mTOR followed by increasing the level of vimentin protein. Osthole suppresses HGF-induced EMT, cell migration, and invasion via repression of the c-Met/Akt/mTOR pathway in human breast cancer cells. Activation of the Erk signaling pathway was not affected by osthole even after a long preincubation when c-Met was no longer maximally activated by HGF. This suggests that the c-Met remaining is sufficient to induce phosphorylation of Erk. Our results are consistent with those of Lee et al., who have shown that luteolin blocked HGF-induced Akt phosphorylation, but only partially affected MAP kinases in hepatoma cells.<sup>28</sup> The PI3K/Akt pathway is indispensable for HGF-induced EMT. Recently, Zhu et al. showed that Akt1 regulated motility and invasion of soft-tissue sarcoma via phosphorylation of vimentin at Ser39.<sup>29</sup> Additionally, EMT-induced vimentin expression positively correlated with Axl, a receptor tyrosine kinase responsible for migration, in clinical samples and breast cancer cell lines.<sup>30</sup> These observations draw attention to EMT-related proteins as therapeutic targets. Significantly, we identified osthole, which could inhibit HGF-induced EMT via down-regulation of phosphorylated Akt and mTOR, and provided a new natural therapeutic compound for breast cancer.

A specific pharmacological inhibitor to FASN, C75, reduced the level of total c-Met protein in MCF-7 breast cancer cells. FASN is the sole enzyme responsible for the de novo synthesis of long-chain unsaturated fatty acids. The addition of exogenous palmitate to the system prevented the C75- and osthole-induced loss of c-Met, further supporting a role of FASN in maintaining c-Met expression levels. Malignant cells have a much greater reliance on de novo synthesized fatty acids as opposed to exogenously derived fatty acids, suggesting that FASN could be a good therapeutic target.<sup>31</sup> The high expression of FASN has been attributed to the maintenance of the lipid supply required by malignant cells. A number of cellular receptors, including c-Met, require localization within ordered lipid rafts for efficient signaling. Lipid rafts are rich in cholesterol and sphingolipids, products generated in tumor cells by FASN. Previous results have suggested that higher FASN activity maintains lipid rafts, which may

help to stabilize levels of c-Met.<sup>25</sup> Our study also provided evidence for a potential link between the FASN activity and the controlling levels of c-Met and that osthole could be a potential therapeutic agent to down-regulate c-Met levels through inhibition of FASN.

## AUTHOR INFORMATION

### Corresponding Author

\*Postal address: Department of Biological Science and Technology, College of Life Sciences, China Medical University, No. 91 Hsueh-Shih Road, Taichung, Taiwan 40402. Phone: +886-4-2205-3366, ext. 2509. Fax: +886-4-2203-1075. E-mail: tdway@mail.cmu.edu.tw.

### Funding Sources

This study was supported by the National Science Council of the Republic of China, Grants NSC 96-2323-B-039-001 and NSC 97-2323-B-039-001. We acknowledge also support (in part) by a grant from the Department of Health (Taiwan), China Medical University Hospital Cancer Research Center of Excellence (DOH100-TD-C-111-005), and grants from China Medical University (CMU99-S-34 and CMU99-TC-02).

## ABBREVIATIONS USED

DMEM, Dulbecco's modified Eagle's medium; DMSO, dimethyl sulfoxide; EGCG, epigallocatechin-3-gallate; EMT, epithelial to mesenchymal transition; FASN, fatty acid synthase; FBS, fetal bovine serum; HGF, hepatocyte growth factor; mTOR, mammalian target of rapamycin; MTT, 3-(4,5-dimethylthiazol-2-yl)-q2,5-diphenyltetrazolium bromide; TGF- $\beta$ , transforming growth factor- $\beta$ .

## REFERENCES

- (1) Gupta, G. P.; Massagué, J. Cancer metastasis: building a framework. *Cell* **2006**, *127*, 679–695.
- (2) Thiery, J. P.; Acloque, H.; Huang, R. Y.; Nieto, M. A. Epithelial mesenchymal transitions in development and disease. *Cell* **2009**, *139*, 871–890.
- (3) Thiery, J. P. Epithelial-mesenchymal transitions in tumour progression. *Nat. Rev. Cancer* **2002**, *2*, 442–454.
- (4) Mani, S. A.; Guo, W.; Liao, M. J.; Eaton, E. N.; Ayyanan, A.; Zhou, A. Y.; Brooks, M.; Reinhard, F.; Zhang, C. C.; Shipitsin, M.; Campbell, L. L.; Polyak, K.; Briskin, C.; Yang, J.; Weinberg, R. A. The epithelial-mesenchymal transition generates cells with properties of stem cells. *Cell* **2008**, *133*, 704–715.
- (5) Polyak, K.; Weinberg, R. A. Transitions between epithelial and mesenchymal states: acquisition of malignant and stem cell traits. *Nat. Rev. Cancer* **2009**, *9*, 265–273.
- (6) Lengyel, E.; Prechtel, D.; Resau, J. H.; Gauger, K.; Welk, A.; Lindemann, K.; Salanti, G.; Richter, T.; Knudsen, B.; Vande Woude, G. F.; Harbeck, N. C-Met overexpression in node-positive breast cancer identifies patients with poor clinical outcome independent of Her2/neu. *Int. J. Cancer* **2005**, *113*, 678–682.
- (7) Ghoussoub, R. A.; Dillon, D. A.; D'Aquila, T.; Rimm, E. B.; Fearon, E. R.; Rimm, D. L. Expression of c-met is a strong independent prognostic factor in breast carcinoma. *Cancer* **1998**, *82*, 1513–1520.
- (8) Birchmeier, C.; Birchmeier, W.; Gherardi, E.; Vande Woude, G. F. Met, metastasis, motility and more. *Nat. Rev. Mol. Cell Biol.* **2003**, *4*, 915–925.
- (9) Taniguchi, T.; Toi, M.; Inada, K.; Imazawa, T.; Yamamoto, Y.; Tominaga, T. Serum concentrations of hepatocyte growth factor in breast cancer patients. *Clin. Cancer Res.* **1999**, *51*, 1031–1034.

- (10) Bigelow, R. L.; Cardelli, J. A. The green tea catechins, (–)-epigallocatechin-3-gallate (EGCG) and (–)-epicatechin-3-gallate (ECG), inhibit HGF/Met signaling in immortalized and tumorigenic breast epithelial cells. *Oncogene* **2006**, *25*, 1922–1930.
- (11) Coleman, D. T.; Bigelow, R.; Cardelli, J. A. Inhibition of fatty acid synthase by luteolin post-transcriptionally down-regulates *c-Met* expression independent of proteosomal/lysosomal degradation. *Mol. Cancer Ther.* **2009**, *8*, 214–224.
- (12) Pan, M. H.; Lai, C. S.; Dushenkov, S.; Ho, C. T. Modulation of inflammatory genes by natural dietary bioactive compounds. *J. Agric. Food Chem.* **2009**, *57*, 4467–4477.
- (13) Zhang, Q.; Qin, L.; He, W.; Van Puyvelde, L.; Maes, D.; Adams, A.; Zheng, H.; De Kimpe, N. Coumarins from *Cnidium monnieri* and their antiosteoporotic activity. *Planta Med.* **2007**, *73*, 13–19.
- (14) Okamoto, T.; Kawasaki, T.; Hino, O. Osthole prevents anti-Fas antibody-induced hepatitis in mice by affecting the caspase-3-mediated apoptotic pathway. *Biochem. Pharmacol.* **2003**, *65*, 677–681.
- (15) Matsuda, H.; Tomohiro, N.; Ido, Y.; Kubo, M. Anti-allergic effects of *cnidium monnieri* fructus (dried fruits of *Cnidium monnieri*) and its major component, osthole. *Biol. Pharm. Bull.* **2002**, *25*, 809–812.
- (16) Luszczki, J. J.; Andres-Mach, M.; Cisowski, W.; Mazol, I.; Glowinski, K.; Czuczwar, S. J. Osthole suppresses seizures in the mouse maximal electroshock seizure model. *Eur. J. Pharmacol.* **2009**, *607*, 107–109.
- (17) Chou, S. Y.; Hsu, C. S.; Wang, K. T.; Wang, M. C.; Wang, C. C. Antitumor effects of osthole from *Cnidium monnieri*: an in vitro and in vivo study. *Phytother. Res.* **2007**, *21*, 226–230.
- (18) Lin, V. C.; Chou, C. H.; Lin, Y. C.; Lin, J. N.; Yu, C. C.; Tang, C. H.; Lin, H. Y.; Way, T. D. Osthole suppresses fatty acid synthase expression in HER2-overexpressing breast cancer cells through modulating Akt/mTOR pathway. *J. Agric. Food Chem.* **2010**, *58*, 4786–4793.
- (19) Way, T. D.; Lin, H. Y.; Kuo, D. H.; Tsai, S. J.; Shieh, J. C.; Wu, J. C.; Lee, M. R.; Lin, J. K. Pu-erh tea attenuates hyperlipogenesis and induces hepatoma cells growth arrest through activating AMP-activated protein kinase (AMPK) in human HepG2 cells. *J. Agric. Food Chem.* **2009**, *57*, 5257–5264.
- (20) Thiery, J. P.; Sleeman, J. P. Complex networks orchestrate epithelial-mesenchymal transitions. *Nat. Rev. Mol. Cell Biol.* **2006**, *7*, 131–142.
- (21) Rong, S.; Segal, S.; Anver, M.; Resau, J. H.; Vande Woude, G. F. Invasiveness and metastasis of NIH 3T3 cells induced by Met-hepatocyte growth factor/scatter factor autocrine stimulation. *Proc. Natl. Acad. Sci. U.S.A.* **1994**, *91*, 4731–4735.
- (22) Jeffers, M.; Schmidt, L.; Nakaigawa, N.; Webb, C. P.; Weirich, G.; Kishida, T.; Zbar, B.; Vande Woude, G. F. Activating mutations for the Met tyrosine kinase receptor in human cancer. *Proc. Natl. Acad. Sci. U.S.A.* **1997**, *94*, 11445–11450.
- (23) Takayama, H.; LaRochelle, W. J.; Sharp, R.; Otsuka, T.; Kriebel, P.; Anver, M.; Aaronson, S. A.; Merlino, G. Diverse tumorigenesis associated with aberrant development in mice overexpressing hepatocyte growth factor/scatter factor. *Proc. Natl. Acad. Sci. U.S.A.* **1997**, *94*, 701–706.
- (24) Wang, R.; Ferrell, L. D.; Faouzi, S.; Maher, J. J.; Bishop, J. M. Activation of the Met receptor by cell attachment induces and sustains hepatocellular carcinomas in transgenic mice. *J. Cell Biol.* **2001**, *153*, 1023–1034.
- (25) Duhon, D.; Bigelow, R. L.; Coleman, D. T.; Steffan, J. J.; Yu, C.; Langston, W.; Kevil, C. G.; Cardelli, J. A. The polyphenol epigallocatechin-3-gallate affects lipid rafts to block activation of the *c-Met* receptor in prostate cancer cells. *Mol. Carcinog.* **2010**, *49*, 739–749.
- (26) Gupta, P. B.; Onder, T. T.; Jiang, G.; Tao, K.; Kuperwasser, C.; Weinberg, R. A.; Lander, E. S. Identification of selective inhibitors of cancer stem cells by high-throughput screening. *Cell* **2009**, *138*, 645–659.
- (27) Vermeulen, L.; De Sousa E Melo, F.; van der Heijden, M.; Cameron, K.; de Jong, J. H.; Borovski, T.; Tuynman, J. B.; Todaro, M.; Merz, C.; Rodermond, H.; Sprick, M. R.; Kemper, K.; Richel, D. J.; Stassi, G.; Medema, J. P. Wnt activity defines colon cancer stem cells and is regulated by the microenvironment. *Nat. Cell Biol.* **2010**, *12*, 468–476.
- (28) Lee, W. J.; Wu, L. F.; Chen, W. K.; Wang, C. J.; Tseng, T. H. Inhibitory effect of luteolin on hepatocyte growth factor/scatter factor-induced HepG2 cell invasion involving both MAPK/ERKs and PI3K/Akt pathways. *Chem.–Biol. Interact.* **2006**, *160*, 123–133.
- (29) Zhu, Q. S.; Rosenblatt, K.; Huang, K. L.; Lahat, G.; Brobey, R.; Bolshakov, S.; Nguyen, T.; Ding, Z.; Belousov, R.; Bill, K.; Luo, X.; Lazar, A.; Dicker, A.; Mills, G. B.; Hung, M. C.; Lev, D. Vimentin is a novel AKT1 target mediating motility and invasion. *Oncogene* **2010**, *30*, 457–470.
- (30) Vuoriluoto, K.; Haugen, H.; Kiviluoto, S.; Mpindi, J. P.; Nevo, J.; Gjerdrum, C.; Tiron, C.; Lorens, J. B.; Ivaska, J. Vimentin regulates EMT induction by Slug and oncogenic H-Ras and migration by governing Axl expression in breast cancer. *Oncogene* **2010**, *30*, 1436–1448.
- (31) Medes, G.; Thomas, A.; Weinhouse, S. Metabolism of neoplastic tissue. IV. A study of lipid synthesis in neoplastic tissue slices in vitro. *Cancer Res.* **1953**, *13*, 27–29.
- (32) Swinnen, J. V.; Van Veldhoven, P. P.; Timmermans, L.; De Schrijver, E.; Brusselmans, K.; Vanderhoydonc, F.; Van de Sande, T.; Heemers, H.; Heys, W.; Verhoeven, G. Fatty acid synthase drives the synthesis of phospholipids partitioning into detergent-resistant membrane microdomains. *Biochem. Biophys. Res. Commun.* **2003**, *302*, 898–903.